0522

Free-Breathing Hepatic Fat Quantification in Children and Infants Using a 3D Stack-Of-Radial Technique: Assessment of Accuracy and Repeatability

Tess Armstrong[1,2], Karrie V. Ly[3], Yu Wang[1,4], Thomas Martin[1,2], Shahnaz Ghahremani[1], Kyunghyun Sung[1,2], Kara L. Calkins[3], and Holden H. Wu[1,2]

[1]Radiological Sciences, University of California Los Angeles, Los Angeles, CA, United States, [2]Physics and Biology in Medicine, University of California Los Angeles, Los Angeles, CA, United States, [3]Pediatrics, Division of Neonatology, David Geffen School of Medicine, University of California Los Angeles, Mattel Children's Hospital, Los Angeles, CA, United States, [4]Biomedical Engineering, Tsinghua University, Beijing, China

Synopsis

Non-alcoholic fatty liver disease (NAFLD) has increasing prevalence in children and early risk factors for NAFLD may be present during infancy. MRI can non-invasively quantify hepatic fat, but current techniques require breath-holding (BH), which is not possible in many children and infants. In this study, a novel free-breathing (FB) 3D stack-of-radial fat quantification technique was developed and evaluated in children and infants. The proposed FB technique achieved accurate and repeatable hepatic fat quantification and improved image quality compared to conventional BH techniques. This FB technique can potentially improve the diagnosis and monitoring of NAFLD in children and infants.

Introduction

Pediatric non-alcoholic fatty liver disease (NAFLD), characterized by hepatic steatosis, is a major health issue with prevalence approaching 38%[1] in obese children. Infants born to mothers with obesity or gestational diabetes can already have increased hepatic fat[2–4] and are at increased risk for NAFLD. NAFLD is diagnosed by liver biopsies[5,6], which are invasive, require anesthesia, and have diagnostic deficiencies[7,8]. Therefore, biopsy is undesired for children. MR spectroscopy is the non-invasive standard for hepatic fat quantification, but is limited by sampling bias and requires a breath-hold (BH)[9,10]. MRI can quantify hepatic fat by calculating spatially-resolved proton-density fat fraction (PDFF) maps[11–13]. However, conventional Cartesian MRI techniques are sensitive to respiratory-motion-induced artifacts and require breath-holding. In children, breath-holding may be limited or not possible[14]. Moreover, breath-holding is not possible in infants. Therefore, the purpose of this study was to evaluate the accuracy and repeatability of a recently developed **free-breathing (FB) 3D stack-of-radial hepatic fat quantification technique**[15] in children and infants, compared to conventional BH techniques.

Methods

FB Radial Sequence A golden-angle ordered RF-spoiled bipolar multiecho gradient echo 3D stack-of-radial sequence with gradient correction (**FB radial**)[15] was customized for pediatric imaging.

Experimental Design Twenty-seven subjects were enrolled in this IRB-approved study: ten healthy pediatric subjects (age=11.5±2.7years, BMI=17.6±2.0kg/m^2), nine NAFLD pediatric subjects (age=14.4±2.2years, BMI=32.6±6.12kg/m^2) and eight infants (age=3.2±2.2months, BMI=18.5±3.4kg/m^2). Informed consent and assent were obtained. FB radial, a four-fold undersampled multiecho gradient echo Cartesian sequence (Cartesian) and CAIPIRINHA[16] reconstruction, and stimulated-echo acquisition mode single-voxel MR spectroscopy with T_2 correction[17] (SVS) were acquired at 3T (Skyra/Prisma, Siemens, Germany) with parameters in **Table 1**. Each sequence was scanned twice in variable order to assess repeatability. A 25mmx25mmx25mm SVS region of interest (ROI) was placed in the liver.

Motion Compensation Self-Navigation (Self-Nav) for FB radial was performed using the cross-correlation of the image projection along z (**Fig. 1a-c**). The mode of the Self-Nav end-expiration time points was chosen as the center of the data acceptance window, whose width was adjusted to accept 40-50% of data.

Reconstruction BH Cartesian[18] and BH SVS[17] PDFF were calculated by scanner software. FB radial images were reconstructed offline[15,19] (**Fig. 1d**) and PDFF was calculated[20–22] with the same multi-peak fat[23] and single R_2*[24–26] signal model as BH Cartesian.

Analysis In children, images were scored for motion artifacts on a 4-point scale (1:non-diagnostic, 2:motion artifacts, 3:minimal motion artifacts, and 4:no motion artifacts). Since infants could not BH, images were scored as either 1 (non-diagnostic) or 2 (diagnostic). The distributions of image scores were compared using McNemar and McNemar-Bowker exact tests. To assess quantification, ROIs were drawn on PDFF maps to correspond to SVS ROIs. FB radial both with and without Self-Nav were evaluated. Linear correlation, Bland-Altman and repeatability analyses were performed in children. Repeatability analysis was performed in infants. $P<0.05$ was considered significant.

Results

Images and PDFF maps are shown for a representative NAFLD pediatric subject (**Figure 3**) and infant (**Figure 4**). The FB radial hepatic PDFF was 2.54%±0.77% in healthy children, 21.61%±13.12% in NAFLD children, and 3.43%±1.22% in infants. In NAFLD children, significantly higher image quality scores were observed for FB radial (2.94±0.42) versus BH Cartesian (2.61±0.78) ($P<0.05$). In infants, image quality scores were significantly higher for FB radial (2.00±0.00) versus FB Cartesian (1.23±0.44) ($P<0.05$). In children, all correlation and concordance coefficients (r and ρ_c) were significant ($P<0.001$) between FB radial (with and without Self-Nav) and BH techniques (**Table 2**). The mean differences (MD) and coefficients of repeatability (CR) were less than 0.5% and 4.1%, respectively, for all comparisons (**Table 2**).

Discussion

FB radial PDFF maps of the entire liver were obtained within scan times of 2-5min for children and 2min for infants. The inherent motion robustness of FB radial resulted in reduced motion artifacts compared to BH Cartesian in NAFLD children and infants. Furthermore, Self-Nav reduced motion-blurring and improved sharpness in FB radial images, particularly for infants who cannot BH or hold still. In infants, MD_{within} was lower for FB radial Self-Nav, potentially improving quantitative repeatability. In children, FB radial Self-Nav had increased streaking due to undersampling, which resulted in higher CR. For pediatric NAFLD subjects, there was one outlier where Self-Nav did not perform well, expanding the limits of agreement when comparing to BH Cartesian. To reduce radial streaking artifacts and improve quantification, advanced reconstruction techniques, such as non-Cartesian parallel imaging[27] or compressed sensing[28], can be incorporated for Self-Nav.

Conclusion

FB radial significantly improves image quality compared to current BH MRI techniques, and can achieve accurate and repeatable quantification of hepatic fat in children and infants without need for breath-holding or sedation. This technique can potentially improve diagnosis and monitoring of NAFLD in children and infants who are not capable of breath-holding.

Acknowledgements

The authors thank Aaron Scheffler, Dr. Joanna Yeh, Barbara Lee, Tammy Floore, Smruthi Murthy, Glen Nyborg, and Sergio Godinez at UCLA for their help with this project. This work acknowledges the use of the ISMRM Fat-Water Toolbox (http://ismrm.org/workshops/FatWater12/data.htm).

References

1. Schwimmer JB, Deutsch R, Kahen T, Lavine JE, Stanley C, Behling C. Prevalence of fatty liver in children and adolescents. Pediatrics 2006;118:1388–93. doi: 10.1542/peds.2006-1212.

2. Brumbaugh DE, Tearse P, Cree-Green M, et al. Intrahepatic fat is increased in the neonatal offspring of obese women with gestational diabetes. J. Pediatr. 2013;162. doi: 10.1016/j.jpeds.2012.11.017.

3. Modi N, Murgasova D, Ruager-Martin R, Thomas EL, Hyde MJ, Gale C, Santhakumaran S, Dore CJ, Alavi A, Bell JD. The influence of maternal body mass index on infant adiposity and hepatic lipid content 2695. Pediatr.Res. 2011;70:287–291. doi: 10.1203/PDR.0b013e318225f9b1.

4. Boney CM, Verma A, Tucker R, Vohr BR. Metabolic Syndrome in Childhood: Association With Birth Weight, Maternal Obesity, and Gestational Diabetes Mellitus. Pediatrics 2005;115:e290–e296. doi: 10.1542/peds.2004-1808.

5. Uppal V, Mansoor S, Furuya KN. Pediatric Non-alcoholic Fatty Liver Disease. Curr. Gastroenterol. Rep. 2016;18. doi: 10.1007/s11894-016-0498-9.

6. Della Corte C, Vajro P, Socha P, Nobili V. Pediatric non-alcoholic fatty liver disease: Recent advances. Clin. Res. Hepatol. Gastroenterol. 2014;38:419–422. doi: 10.1016/j.clinre.2014.02.008.

7. Tapper EB, Lok AS-F. Use of Liver Imaging and Biopsy in Clinical Practice. N. Engl. J. Med. 2017;377:756–768. doi: 10.1056/NEJMra1610570.

8. Sumida Y, Nakajima A, Itoh Y. Limitations of liver biopsy and non-invasive diagnostic tests for the diagnosis of nonalcoholic fatty liver disease/nonalcoholic steatohepatitis. World J. Gastroenterol. 2014;20:475–485. doi: 10.3748/wjg.v20.i2.475.

9. Loomba R, Sirlin CB, Schwimmer JB, Lavine JE. Advances in pediatric nonalcoholic fatty liver disease. Hepatology 2009;50:1282–93. doi: 10.1002/hep.23119.

10. Lee SS, Park SH. Radiologic evaluation of nonalcoholic fatty liver disease. World J. Gastroenterol. 2014;20:7392–7402. doi: 10.3748/wjg.v20.i23.7392.

11. Meisamy S, Hines CDG, Hamilton G, Sirlin CB, McKenzie CA, Yu H, Brittain JH, Reeder SB. Quantification of hepatic steatosis with T1-independent, T2-corrected MR imaging with spectral modeling of fat: blinded comparison with MR spectroscopy. Radiology 2011;258:767–775. doi: 10.1148/radiol.10100708.

12. Hines CDG, Yu H, Shimakawa A, McKenzie CA, Brittain JH, Reeder SB. T1 independent, T2* corrected MRI with accurate spectral modeling for quantification of fat: Validation in a fat-water-SPIO phantom. J. Magn. Reson. Imaging 2009;30:1215–1222. doi: 10.1002/jmri.21957.

13. Achmad E, Yokoo T, Hamilton G, et al. Feasibility of and agreement between MR imaging and spectroscopic estimation of hepatic proton density fat fraction in children with known or suspected nonalcoholic fatty liver disease. Abdom. Imaging 2015;40:3084–3090. doi: 10.1007/s00261-015-0506-9.

14. Chavhan GB, Babyn PS, Vasanawala SS. Abdominal MR imaging in children: motion compensation, sequence optimization, and protocol organization. Radiographics 2013;33:703–719. doi: 10.1148/rg.333125027.

15. Armstrong T, Dregely I, Stemmer A, Han F, Natsuaki Y, Sung K, Wu HH. Free-breathing liver fat quantification using a multiecho 3D stack-of-radial technique. Magn. Reson. Med. 2017. doi: 10.1002/mrm.26693.

16. Breuer FA, Blaimer M, Heidemann RM, Mueller MF, Griswold MA, Jakob PM. Controlled aliasing in parallel imaging results in higher acceleration (CAIPIRINHA) for multi-slice imaging. Magn. Reson. Med. 2005;53:1–8. doi: 10.1002/mrm.20401.

17. Pineda N, Sharma P, Xu Q, Hu X, Vos M, Martin DR. Measurement of hepatic lipid: high-speed T2-corrected multiecho acquisition at 1H MR spectroscopy--a rapid and accurate technique. Radiology 2009;252:568–576. doi: 10.1148/radiol.2523082084.

18. Zhong X, Nickel MD, Kannengiesser SAR, Dale BM, Kiefer B, Bashir MR. Liver fat quantification using a multi-step adaptive fitting approach with multi-echo GRE imaging. Magn. Reson. Med. 2014;72:1353–1365. doi: 10.1002/mrm.25054.

19. Walsh DO, Gmitro AF, Marcellin MW. Adaptive reconstruction of phased array MR imagery. Magn. Reson. Med. 2000;43:682–690. doi: 10.1002/(SICI)1522-2594(200005)43:5<682::AID-MRM10>3.0.CO;2-G.

20. Hernando D, Kellman P, Haldar JP, Liang Z-P. Robust water/fat separation in the presence of large field inhomogeneities using a graph cut algorithm. Magn. Reson. Med. 2010;63:79–90. doi: 10.1002/mrm.22177.

21. ISMRM Fat Water Toolbox. 2012.

22. Gleich DF. Models and Algorithms for PageRank Sensitivity. Stanford University; 2009.

23. Ren J, Dimitrov I, Sherry AD, Malloy CR. Composition of adipose tissue and marrow fat in humans by 1H NMR at 7 Tesla. J. Lipid Res. 2008;49:2055–2062. doi: 10.1194/jlr.D800010-JLR200.

24. Horng DE, Hernando D, Hines CDG, Reeder SB. Comparison of R2* correction methods for accurate fat quantification in fatty liver. J. Magn. Reson. Imaging 2013;37:414–22. doi: 10.1002/jmri.23835.

25. Horng DE, Hernando D, Reeder SB. Quantification of liver fat in the presence of iron overload. J. Magn. Reson. Imaging [Internet] 2017. doi: 10.1002/jmri.25382.

26. Yu H, Shimakawa A, McKenzie CA, Brodsky E, Brittain JH, Reeder SB. Multiecho water-fat separation and simultaneous R2* estimation with multifrequency fat spectrum modeling. Magn. Reson. Med. 2008;60:1122–34. doi: 10.1002/mrm.21737.

27. Uecker M, Lai P, Murphy MJ, Virtue P, Elad M, Pauly JM, Vasanawala SS, Lustig M. ESPIRiT - An eigenvalue approach to autocalibrating parallel MRI: Where SENSE meets GRAPPA. Magn. Reson. Med. 2014;71:990–1001. doi: 10.1002/mrm.24751.

28. Benkert T, Feng L, Sodickson DK, Chandarana H, Block KT. Free-Breathing Volumetric Fat/Water Separation by Combining Radial Sampling, Compressed Sensing, and Parallel Imaging. Magn. Reson. Med. 2016. doi: 10.1002/mrm.26392.

Figures

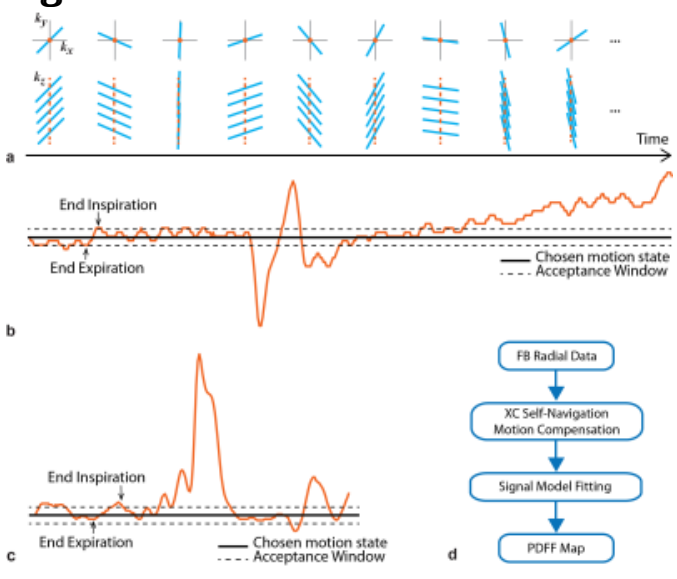

Figure 1: (a) 3D stack-of-radial trajectory. Radial readouts are acquired along k_z before rotating by the golden angle. The Fourier transform of the center of k-space for each angle is compared using cross-correlation (XC) to determine the Self-Nav signal for **(b)** children and **(c)** infants. The mode of each end expiration position was the chosen motion state and the acceptance window width was adjusted to accept 40-50% of the radial angles. **(d)** The Self-Nav compensated data then undergoes signal model fitting to calculate proton-density fat fraction (PDFF) maps.

Imaging Parameters	BH Cartesian (Pediatric)	FB Radial (Pediatric)	FB Radial (Infant)
TE (ms)	1.23, 2.46, 3.69, 4.92, 6.15, 7.38	1.23, 2.46, 3.69, 4.92, 6.15, 7.38	1.23, 2.46, 3.69, 4.92, 6.15, 7.38
ΔTE (ms)	1.23	1.23	1.23
TR (ms)	8.85	8.85	8.85
Matrix (N_x x N_y)	160-288 x 160-288	160-288 x 160-288	96-128 x 96-128
Field of View (mm_x x mm_y)	280-500 x 280-500	280-500 x 280-500	150-200 x 150-200
Resolution (mm_x x mm_y)	1.67-1.94 x 1.67-1.94	1.67-1.94 x 1.67-1.94	1.67 x 1.67
Slice Thickness (mm)	5	5	3
Number of Slices	20-40	36-52	40
Radial Spokes	N/A	252-453	151-202
Flip Angle (degrees)	5	5	5
Bandwidth (Hz/pixel)	1080-1160	1080-1160	1150-1155
Acceleration Factor	4	1	1
Scan Time (min:s)	0:16-0:25	2:09*-4:43*	1:38*-2:00*

Table 1: Representative sequence parameters for pediatric liver experiments. A slice-oversampling factor of 18-25% was used for the acquisitions. Imaging parameters for free-breathing (FB) radial and breath-hold (BH) Cartesian were matched as much as possible for each subject. The number of slices was adjusted depending on scan time and the subjects' BH ability. *The FB radial gradient calibration scan time of 31-45s for pediatric subjects and 34s for infants is included.

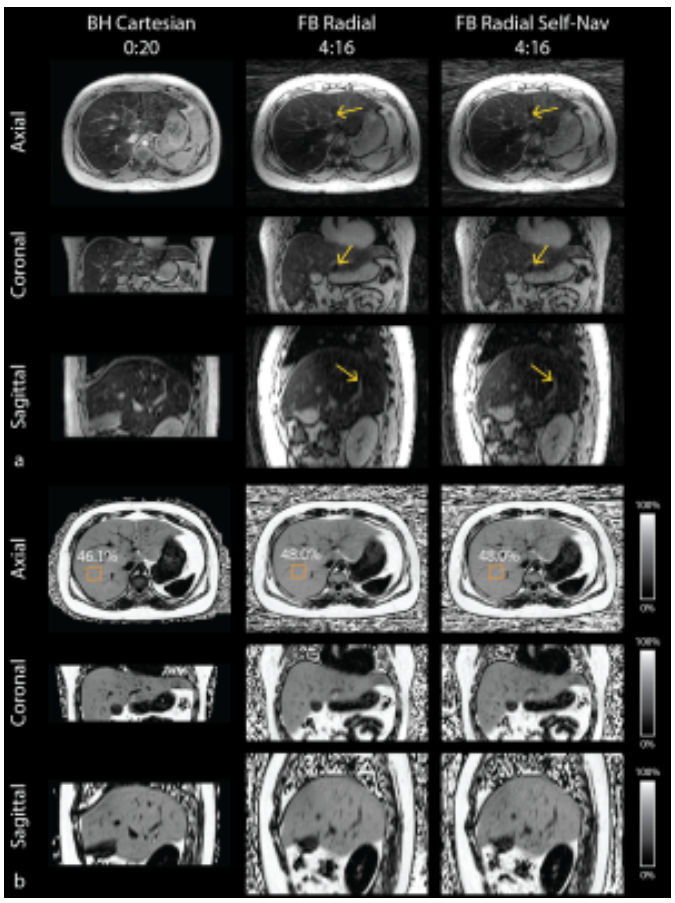

Figure 2: Representative results from a NAFLD pediatric subject. BH Cartesian, FB radial, and FB radial Self-Nav **(a)** liver images at TE = 1.23ms and **(b)** PDFF maps in axial, coronal reformat, and sagittal reformat orientations. This subject's self-navigation signal was shown in **Figure 1b**. Radial image sharpness is improved using Self-Nav (yellow arrows). For this subject, SVS PDFF was 48.4%. The scan time for each technique is reported as (minutes:seconds). Since FB radial was reconstructed offline, there are differences in the image intensity between FB radial and BH Cartesian caused by uncompensated coil sensitivity profile differences.

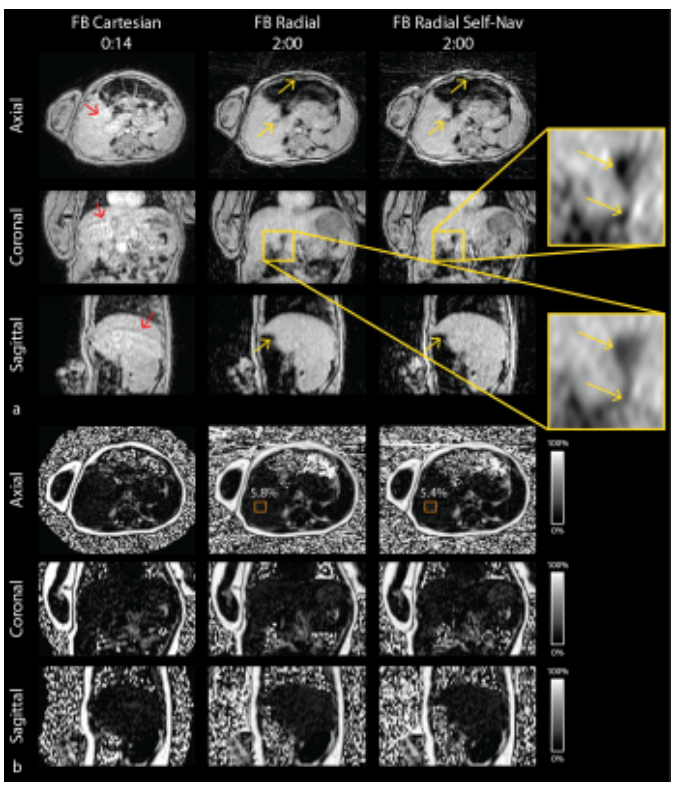

Figure 3: Representative infant results. FB Cartesian, FB radial, and FB radial Self-Nav **(a)** liver images at TE = 1.23ms and **(b)** PDFF maps in axial, coronal reformat, and sagittal reformat orientations. This infant's self-navigation signal was shown in **Figure 1c**. Significant motion artifacts are observed on FB Cartesian images (red arrows) and radial image sharpness is improved using Self-Nav (yellow arrows). For this subject, SVS PDFF was 5.8%. The scan time for each technique is reported as (minutes:seconds).

Hepatic Fat Quantification Accuracy in Pediatric Subjects				
	r	ρ_c	MD (%)	LoA (%)
FB Radial vs. BH Cartesian	0.9953*	0.9934*	0.6363%	[-1.9718%, 3.2444%]
FB Radial vs. BH SVS	0.9967*	0.9954*	0.6241%	[-1.7050%, 2.9532%]
FB Radial Self-Nav vs. BH Cartesian	0.9268*	0.9052*	2.3879%	[-8.2122%, 12.9880%]
FB Radial Self-Nav vs. BH SVS	0.9974*	0.9940*	1.1359%	[-0.8849%, 3.1566%]

Hepatic Fat Quantification Repeatability Analysis in Pediatric Subjects		
	MD_{within} (%)	CR (%)
FB Radial	-0.2558%	1.5341%
FB Radial Self-Nav	0.4063%	4.0511%
BH Cartesian	-0.0911%	0.8897%
BH SVS	-0.2969%	3.7408%

Hepatic Fat Quantification Repeatability Analysis in Infant Subjects		
	MD_{within} (%)	CR (%)
FB Radial	-0.2163%	1.9618%
FB Radial Self-Nav	-0.1625%	2.0828%

Table 2: The linear correlation, Bland-Altman and repeatability analyses results. Pearson's correlation coefficient (r), Lin's concordance coefficient (ρ_c), mean differences (MD) between techniques, Limits of agreement (LoA) between techniques, is reported for each comparison. For repeatability, the mean differences within (MD_{within}) and coefficient of repeatability (CR) is reported. *Indicates statistical significance with $P < 0.001$.